



Microscopic model for ultrafast magnetization dynamics of multisublattice magnets

A. J. Schellekens and B. Koopmans

Department of Applied Physics, Center for NanoMaterials (cNM), Eindhoven University of Technology, P.O. Box 513, 5600 MB Eindhoven, The Netherlands

(Received 29 October 2012; revised manuscript received 6 December 2012; published 25 January 2013)

We introduce a microscopic model to describe the ultrafast response of magnetic materials with two sublattices to heating by a femtosecond laser pulse. Even though the model is based on a set of simple Hamiltonians, it readily reproduces experimental observations such as ultrafast reversal of ferrimagnets and delayed demagnetization of one sublattice in ferromagnetic alloys. The calculations give insight into the microscopic mechanisms and thermodynamics governing the complex dynamics of these multisublattice magnets.

DOI: [10.1103/PhysRevB.87.020407](https://doi.org/10.1103/PhysRevB.87.020407)

PACS number(s): 75.78.Jp, 75.60.Jk, 75.50.Gg, 75.50.Bb

Controlling the magnetic state of ferromagnetic materials by femtosecond laser pulses has drawn significant attention from the scientific community since the first pioneering experiments by Beaurepaire *et al.*¹ In these experiments it was shown that the magnetization of ferromagnetic nickel can be quenched on subpicosecond time scales. This discovery led to intense theoretical^{2–9} and experimental^{10–16} investigations on the origin of these ultrafast magnetization dynamics, however, the dominant microscopic mechanism is still under debate.

Parallel to the research on the dynamics of homogeneous ferromagnets, more exotic materials were being investigated. A breakthrough in the field was made by Stanciu *et al.*,¹⁷ who have shown that the direction of the magnetization of the sublattices in the ferrimagnetic alloy GdFeCo can be changed by the use of a femtosecond laser pulse and a small applied field. Recently, the origin of this magnetization reversal has been unraveled by separately measuring the dynamics of the Gd and FeCo sublattices.¹⁸ It was concluded that a different heating efficiency of the two sublattices puts the system in a strong nonequilibrium state, making it possible for the magnetization to switch its orientation. This result was corroborated by further experiments and atomistic spin simulations, showing that even without an external field the mutual orientation of the sublattices can be switched,¹⁹ paving the way for all optical recording.

Recently, it was shown that also the magnetic moments of Ni and Fe in permalloy show strong nonequilibrium dynamics after pulsed laser excitation.²⁰ Element-specific measurements show that the demagnetization of Ni is delayed with respect to Fe, which is a surprising observation considering the large hybridization of the electronic states around the Fermi level in permalloy. This begs the question what microscopic processes govern these different dynamics and under which conditions they occur.

In this Rapid Communication, we derive a model describing the longitudinal relaxation of magnetic materials with two sublattices. The main difference between existing methods in the literature^{21,22} is that it is based on microscopic scattering Hamiltonians. Our approach finds its origin in the microscopic 3 temperature model (M3TM),⁶ which describes three interacting subsystems of (spinless) electrons, phonons, and $S = 1/2$ spin excitations. We extend the model to $S = N/2$, introduce more than one spin system, and drop the restriction that the spin systems are in internal equilibrium. First the

response of a ferrimagnetic material is investigated, where the two sublattices are aligned antiparallel. Experimentally observed switching of the sublattices through a transient ferromagnetic state is readily reproduced. Second, the same model is applied to permalloy, where the Fe and Ni sublattices are coupled ferromagnetically. It is demonstrated that, under certain assumptions, a delay in the demagnetization of one of the sublattices can be observed indeed, again corresponding to the experimental observations. The nature of the assumptions reveals important information on the microscopic processes governing ultrafast magnetization dynamics in these strongly coupled ferromagnetic alloys.

The equations of motion we derive are aimed to be the simplest microscopic description of a multisublattice magnet, but accurate enough to keep contact with experimental observations. To this end, while we treat separate spin subsystems, for simplicity we let them interact with only one common electron system, which is assumed to be a noninteracting Fermi sea of spinless fermions with a constant density of states D_F around the Fermi level. The phonon bath is described by a Debye model, i.e., by assuming a linear dispersion relation for D_p phonon modes up to a cutoff energy $E_D = k_B T_D$. The two spin systems m_i are described by $2S + 1$ discrete energy levels that are split by an energy J_{ex} , where S is the spin quantum number. This yields the following Hamiltonians for the electron, phonon, and i th spin systems, respectively:

$$\mathcal{H}_e = \frac{1}{ND_f} \sum_k \frac{k^2}{2m} c_k^\dagger c_k, \quad (1)$$

$$\mathcal{H}_p = \sum_q^{3D_p} \hbar \omega_q \left(\frac{1}{2} + a_q^\dagger a_q \right), \quad (2)$$

$$\mathcal{H}_{s,i} = J_{ex,i} \sum_j^{ND_{s,i}} S_{z,i,j}, \quad (3)$$

where c_k^\dagger (c_k) describes the creation (annihilation) of an electron in the state k , a_q^\dagger (a_q) are similar operators for phonons in the state q , $D_{s,i}$ is the average atomic spin density, and $S_{z,i,j}$ is the z spin operator.

For the spin system a Weiss mean-field approach is used, where the exchange splitting of the discrete energy levels is

given by

$$J_{\text{ex},1} = (\gamma_{1,1}m_1 + \gamma_{1,2}m_2)/S_1, \quad (4)$$

$$J_{\text{ex},2} = (\gamma_{2,2}m_2 + \gamma_{1,2}m_1)/S_2, \quad (5)$$

where m_1 and m_2 are the normalized magnetizations of the two sublattices, and $\gamma_{1,1}$, $\gamma_{2,2}$, and $\gamma_{1,2}$ are the Weiss molecular field constants, which are related to the intra- and intersublattice exchange energies, respectively. When $\gamma_{1,2}$ is positive (negative) the sublattices are ferromagnetically (antiferromagnetically) coupled.

To describe the interactions between the subsystems the scattering Hamiltonians have to be introduced. First of all, it is assumed that $e-e$ and $p-p$ scattering are instantaneous, hence the e and p systems are in internal equilibrium at all times. Second, $e-p$ scattering is taken into account within the random- k approximation. Like in the M3TM, phonon-assisted Elliott-Yafet spin flips couple the spin system to the electronic heat bath, transferring the angular momentum between the spin and phonon subsystems. Finally, exchange scattering is added,²³ where in an interband $e-e$ scattering event angular momentum is transferred between the two magnetic sublattices. This yields the following scattering Hamiltonians:

$$\mathcal{H}_{\text{ep}} = \frac{\lambda_{\text{ep}}}{N} \sum_k \sum_{k'} \sum_q^{ND_p} c_k^\dagger c_k (a_q^\dagger + a_q), \quad (6)$$

$$\mathcal{H}_{\text{eps},i} = \sqrt{\frac{a_{\text{sf},i}}{D_{s,i}}} \frac{\lambda_{\text{ep}}}{N^{3/2}} \sum_k \sum_{k'} \sum_q^{ND_p} \sum_j^{ND_s} c_k^\dagger c_k (a_q^\dagger + a_q) (s_{i,j,+} + s_{i,j,-}), \quad (7)$$

$$\mathcal{H}_{\text{ex}} = \frac{\lambda_{\text{ex}}}{N^3} \sum_k \sum_{k'} \sum_{k''} \sum_{k'''}^{ND_{s,1}} \sum_v \sum_w^{ND_{s,2}} c_{k'''}^\dagger c_{k''}^\dagger c_{k'} c_k (s_{1,+v} s_{2,-w} + s_{1,-v} s_{2,+w}), \quad (8)$$

where $s_{1,+v}$ ($s_{1,-v}$) is a raising (lowering) operator for the v th spin of the first spin system, λ_{ep} and λ_{ex} the matrix elements for $e-p$ and exchange scattering, and a_{sf} the probability of a phonon-mediated Elliott-Yafet spin flip. Compared to the original M3TM, an extra microscopic parameter λ_{ex} is introduced into the model. This matrix element is the interatomic exchange integral of the spins on the different atoms of the sublattices, which is typically of the order of 10–100 meV. Although it has the same origin as the intersublattice Weiss molecular field constant $\gamma_{1,2}$, it cannot be directly related to this mean-field exchange. Therefore, λ_{ex} is treated as a free parameter. Finally, we would like to stress that, even though all Hamiltonians are microscopic in spirit, they are a rather phenomenological description of a far more complex system.

The scattering Hamiltonians can be evaluated by using Fermi's golden rule, which yields a system of coupled Boltzmann scattering equations for the electron temperature T_e , the phonon temperature T_p , and the occupation of the discrete energy levels for the two spin systems. An overview of the resulting model is depicted in Fig. 1. In Figs. 1(a) and 1(b) the energy and angular momentum flow between the subsystems is depicted. Note that the total amount of energy in the system is conserved at all times. Additions to the basic

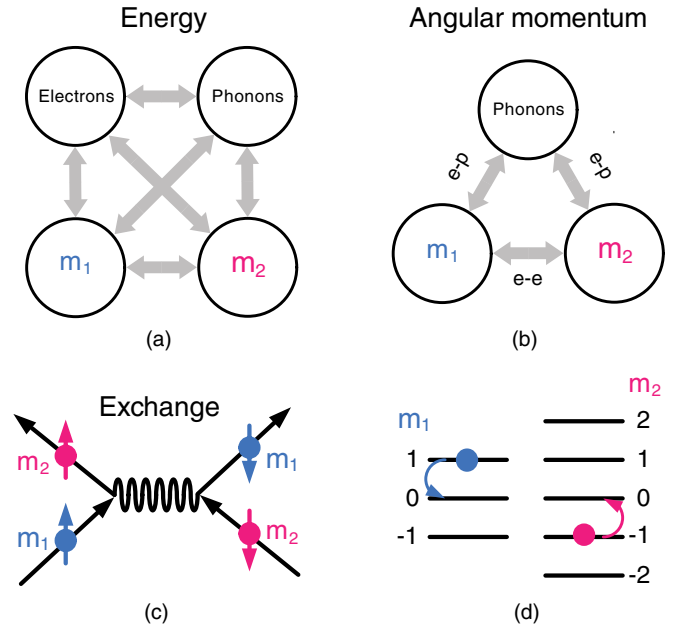


FIG. 1. (Color online) Schematic overview of the model. (a) Energy flow between the subsystems. (b) Flow of the angular momentum between the subsystems. Due to exchange scattering, the angular momentum can be transported between the two magnetic sublattices. Both sublattices can exchange angular momentum with the lattice by $e-p$ scattering. (c) Spin-flip event due to $e-e$ scattering, transferring angular momentum from one sublattice to the other. (d) Change of occupation of the discrete energy levels due to the exchange scattering event depicted in (c).

M3TM model⁶ are that (i) an exchange scattering mechanism is taken into account, which is schematically depicted in Figs. 1(c) and 1(d), and (ii) there are two spin sublattices which are neither in internal equilibrium nor in equilibrium with respect to each other. The main difference between the here derived model and the atomistic Landau-Lifschitz-Gilbert^{18,19} and Landau-Lifschitz-Bloch (LLB) approach⁹ is that the coupling of the spin system to the electron and phonon baths is derived from microscopic scattering Hamiltonians instead of a phenomenological coupling constant. We do note that replacing this phenomenological coupling constant by a parameter derived from the same microscopic scattering Hamiltonians could yield similar results, which has been shown to be the case for the LLB and M3TM.⁹

All ingredients to calculate the magnetization dynamics of the sublattices due to femtosecond laser pulse heating have now been introduced. Next we proceed to check whether the model can reproduce the ultrafast reversal of a ferrimagnet due to a fs heat pulse. The aim of the calculations is not to reproduce the experimental observations as closely as possible, but to show that the model qualitatively yields similar dynamics. To this extent we introduce the most simple fictitious ferrimagnet, namely, one with a 1:1 atomic ratio and respective spin quantum numbers $S_1 = 1/2$ and $S_2 = 1$, representing the transition metal $3d$ and rare-earth $4f$ spins, respectively. The indirect exchange of these moments, mediated by $4f-5d$ intra-atomic exchange and $3d-5d$ hybridization,²⁴ is for simplicity replaced by a single interatomic exchange. The molecular field constants are $\gamma_{1,1} = 4\gamma_{2,2} = -4\gamma_{1,2} = 138$ meV. The other

TABLE I. Microscopic parameters used in the calculations. The magnetic parameters are mentioned in the main text.

	D_F	D_p	D_s	T_D	λ_{ep}	$\lambda_{ex,0}$	a_{sf}
Ferrimagnet	3/eV	3	1/1	400 K	20 meV	25 meV	0.1
Ferromagnet	3/eV	3	0.8/0.2	400 K	20 meV	70 meV	0.1

microscopic parameters are given in Table I. We would like to stress that these parameters are very realistic for ferromagnetic materials and similar to the ones reported earlier.⁶ Finally, the laser pulse is assumed to have a Gaussian profile with a standard deviation of 50 fs.

Figure 2(a) displays the resulting equilibrium magnetization as a function of temperature. The symbols are the equilibrium values obtained by solving the derived differential equations for $T_e = T_p = T_{\text{ambient}}$, whereas the lines are calculated using the Weiss model. The molecular field constants are chosen such that the compensation temperature T_{comp} of the ferrimagnet is slightly larger than room temperature, as in the first experiments.¹⁷ In Figs. 2(b) and 2(c) the typical time evolution of the electron (phonon) temperature T_e (T_p) and the magnetic moments on the sublattices are displayed, respectively, however, in the calculations exchange scattering is neglected by setting λ_{ex} to zero. Just as in the experiments, the sublattice with the strongest exchange coupling and smallest magnetic moment, M_1 , demagnetizes more rapidly. This is in line with predictions of the original M3TM, where the demagnetization rate is proportional to the intrasublattice exchange and inversely proportional to the atomic magnetic moment.⁶

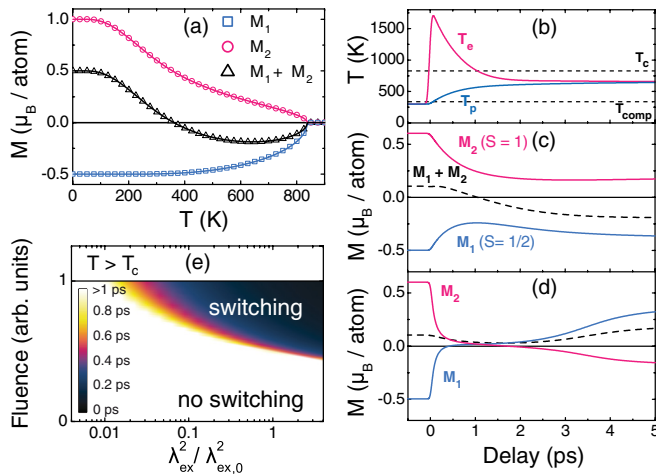


FIG. 2. (Color online) (a) Equilibrium magnetic moments of the sublattices of the fictitious ferrimagnet as a function of temperature. The lines are calculated using the self-consistent mean-field approach, whereas the symbols represent the equilibrium values in the Boltzmann scattering equations. (b) Electron and phonon dynamics for the fluence used in (c) and (d). (c) Ultrafast demagnetization of the sublattices neglecting exchange scattering. (d) Ultrafast demagnetization for the same microscopic parameters as in (c), but allowing for an angular momentum transfer between the sublattices by exchange scattering. (e) Switching time as a function of fluence and the matrix element for exchange scattering.

Next, in contrast to the calculation in Fig. 2(c), exchange scattering is turned on, allowing for an angular momentum transfer between the subsystems. The corresponding calculations, while keeping other microscopic parameters fixed, are displayed in Fig. 2(d). The main difference from Fig. 2(c) is that the demagnetization rates of both sublattices are enhanced significantly due to the extra transport channel for the angular momentum. While the electron temperature is larger than T_C , one would expect that the magnetization of the sublattices would be fully quenched. However, an unexpected ferromagnetic alignment of the sublattices is observed. Since M_1 (originally in the negative direction) demagnetizes more rapidly than M_2 , it reaches zero while M_2 still has a relatively large (positive) magnetic moment. M_2 will now be further quenched by exchange scattering, however, this inevitably leads to a slightly positive value of M_1 and thus a temporary ferromagnetic state. When the electron system cools below T_C due to equilibration with the phonons after ≈ 1 ps, the magnetization of the sublattice coupled most strongly to the electrons, i.e., M_1 , starts growing to larger positive values. Then, finally, the antiferromagnetic coupling with M_2 acts as the driving force to switch the orientation of M_2 from positive to negative.

In the model one parameter is introduced that cannot be easily obtained from experiments, which is λ_{ex} . To show that switching does not depend strongly on this parameter but is in fact very robust, we plot the switching time as a function of laser fluence and λ_{ex}^2 in Fig. 2(e). The switching time is defined as the delay time where M_1 and M_2 cross. Switching is observed if λ_{ex}^2 is sufficiently large, and the laser fluence is larger than a certain threshold value. The range where switching occurs is reasonably large, and for every value of $\lambda_{ex}^2 / \lambda_{ex,0}^2 > 0.2$ there is a fluence where the sublattices change their mutual orientation. For fluences larger than 1 (arb. units) the final temperature after laser pulse excitation is larger than T_C , hence no switching occurs.

After verifying that ultrafast switching of antiferromagnetically coupled sublattices can be described by the presented model, we will investigate the magnetization dynamics of two ferromagnetically coupled sublattices as recently studied experimentally by Mathias *et al.*²⁰ Here it was shown that the quenching of the (average) magnetic moment on the Ni atoms in permalloy is delayed with respect to the moments on the Fe atoms. To calculate the magnetization dynamics of permalloy with the introduced model, the exchange coupling between the sublattices is assumed to be ferromagnetic. Furthermore, because the electronic states around the Fermi level of Ni and Fe are strongly hybridized, it is assumed that the inter- and intrasublattice exchange interactions are identical, giving the same temperature dependent equilibrium properties of the sublattices.

For the calculations a fictitious ferromagnetic alloy resembling permalloy is used, which is an 80-20 mixture of Ni (M_1) and Fe (M_2) with a Curie temperature of 800 K. The spin-flip rate of M_1 is chosen to be four times smaller than that of M_2 , hence without any exchange coupling between the sublattices M_1 demagnetizes four times slower due to e - p scattering. The other microscopic parameters used, which are chosen to be very similar to the ferrimagnetic case, are given in Table I.

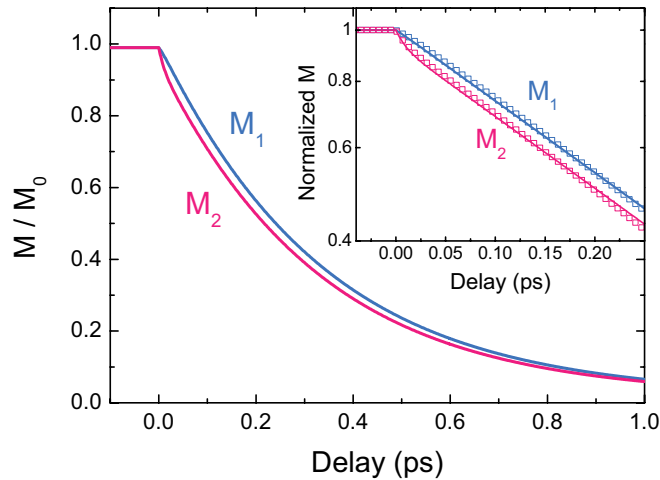


FIG. 3. (Color online) Calculated element-specific demagnetization of the ferromagnetic alloy as a function of delay time. In the inset the normalized demagnetization is plotted on a semilogarithmic scale, where the dots are the model calculations and the lines fits with a simple model.

Results of the calculations are displayed in Fig. 3, where the magnetizations of the sublattices M_1 and M_2 are plotted as a function of time after laser pulse excitation. Note that it is assumed that heating by the laser pulse is instantaneous, heating the electron system to 1600 K at $t = 0$. The calculations show that for the parameters used, M_2 and M_1 demagnetize at approximately the same rate, but M_1 is delayed with respect to M_2 . This is in full agreement with the experimental results.²⁰ The same mechanism as in the ferrimagnetic alloy is at play, i.e., transfer of the angular momentum between the subsystems by exchange scattering brings the total system closer to equilibrium, slowing down the demagnetization of M_2 but increasing the demagnetization rate of M_1 until both rates are approximately equal.

To exemplify this delayed demagnetization, the normalized magnetizations $(M - M_{\min})/(M_0 - M_{\min})$ of both sublattices are plotted on a semilogarithmic scale in the inset of Fig. 3.

The data is fitted by the following simple model:

$$\frac{dm_1}{dt} = -\frac{m_1}{\tau_1} - \frac{D_{s2}}{D_{s1}} \frac{m_1 - m_2}{\tau_{\text{ex}}}, \quad (9)$$

$$\frac{dm_2}{dt} = -\frac{m_2}{\tau_2} - \frac{D_{s1}}{D_{s2}} \frac{m_2 - m_1}{\tau_{\text{ex}}}, \quad (10)$$

where τ_1 and τ_2 are the time constants for demagnetization of the two individual sublattices, while τ_{ex} is the time scale of the exchange interaction. Note that this fit function is almost identical to the one used by Mathias *et al.*,²⁰ except the fraction of the atomic spin densities is added to the exchange interaction term, as the total angular momentum should be conserved in the exchange scattering process. It can be observed from the inset of Fig. 3 that the simple model fits the data reasonable well, and $\tau_{\text{ex}} = 44 \pm 2$ fs is obtained from the fits. Furthermore, τ_1/τ_2 is found to be ≈ 4 . We can thus conclude that the derived microscopic model shows similar dynamics to the experimental ones when assuming that the magnetic moments of the Ni atoms are less strongly coupled to the electronic system compared to Fe. The origin of such a difference, which is rather unexpected due to the large hybridization of the electronic system, remains to be elucidated.

To conclude, we have introduced a simple microscopic model to describe the ultrafast dynamics of magnetic materials with ferro- or antiferromagnetically coupled sublattices. Both ultrafast switching of a ferrimagnet and the magnetization dynamics of a strongly hybridized ferromagnetic alloy are readily reproduced by using realistic values for the microscopic material parameters. Although within the present Rapid Communication we only discussed two cases where the two spin sublattices are associated with different atomic positions, our approach is much more general, and can be extended easily to cases with more sublattices, or sublattices representing different orbitals on the same atom. Treating the coupled dynamics of d and f magnetic moments in rare-earth ferromagnets would provide an intriguing example thereof.

This work was supported by the Foundation for Fundamental Research on Matter (FOM), which is part of the Netherlands Organization for Scientific Research (NWO).

¹E. Beaupaire, J. C. Merle, A. Daunois, and J. Y. Bigot, *Phys. Rev. Lett.* **76**, 4250 (1996).

²G. P. Zhang and W. Hübner, *Phys. Rev. Lett.* **85**, 3025 (2000).

³B. Koopmans, J. J. M. Ruigrok, F. Dalla Longa, and W. J. M. de Jonge, *Phys. Rev. Lett.* **95**, 267207 (2005).

⁴N. Kazantseva, U. Nowak, R. W. Chantrell, J. Hohlfeld, and A. Rebei, *Europhys. Lett.* **81**, 27004 (2007).

⁵M. Krauss, T. Roth, S. Alebrand, D. Steil, M. Cinchetti, M. Aeschlimann, and H. C. Schneider, *Phys. Rev. B* **80**, 180407 (2009).

⁶B. Koopmans, G. Malinowski, F. Dalla Longa, D. Steiauf, M. Fähnle, T. Roth, M. Cinchetti, and M. Aeschlimann, *Nat. Mater.* **9**, 259 (2010).

⁷M. Battiato, K. Carva, and P. M. Oppeneer, *Phys. Rev. Lett.* **105**, 027203 (2010).

⁸K. Carva, M. Battiato, and P. M. Oppeneer, *Phys. Rev. Lett.* **107**, 207201 (2011).

⁹U. Atxitia and O. Chubykalo-Fesenko, *Phys. Rev. B* **84**, 144414 (2011).

¹⁰B. Koopmans, M. van Kampen, J. T. Kohlhepp, and W. J. M. de Jonge, *Phys. Rev. Lett.* **85**, 844 (2000).

¹¹H.-S. Rhie, H. A. Dürr, and W. Eberhardt, *Phys. Rev. Lett.* **90**, 247201 (2003).

¹²M. Djordjevic and M. Müntenberg, *Phys. Rev. B* **75**, 012404 (2007).

¹³C. Stamm, T. Kachel, N. Pontius, R. Mitzner, T. Quast, K. Hollmack, S. Khan, C. Lupulescu, E. F. Aziz, M. Wietstruk, H. A. Dürr, and W. Eberhardt, *Nat. Mater.* **6**, 740 (2007).

¹⁴E. Carpene, E. Mancini, C. Dallera, M. Brenna, E. Puppini, and S. De Silvestri, *Phys. Rev. B* **78**, 174422 (2008).

- ¹⁵G. M. Müller, J. Walowski, M. Djordjevic, G-X. Miao, A. Gupta, A. V. Ramos, K. Gehrke, V. Moshnyaga, K. Samwer, J. Schmalhorst, A. Thomas, A. Hütten, G. Reiss, J. S. Moodera, and M. Münzenberg, *Nat. Mater.* **8**, 56 (2009).
- ¹⁶D. Steil, S. Alebrand, T. Roth, M. Krauss, T. Kubota, M. Oogane, Y. Ando, H. C. Schneider, M. Aeschlimann, and M. Cinchetti, *Phys. Rev. Lett.* **105**, 217202 (2010).
- ¹⁷C. D. Stanciu, A. Tsukamoto, A. V. Kimel, F. Hansteen, A. Kirilyuk, A. Itoh, and Th. Rasing, *Phys. Rev. Lett.* **99**, 217204 (2007).
- ¹⁸I. Radu, K. Vahaplar, C. Stamm, T. Kachel, N. Pontius, H. A. Dürr, T. A. Ostler, J. Barker, R. F. L. Evans, R. W. Chantrell, A. Tsukamoto, A. Itoh, A. Kirilyuk, T. Rasing, and A. V. Kimel, *Nature (London)* **472**, 7342 (2011).
- ¹⁹T. A. Ostler, J. Barker, R. F. L. Evans, R. W. Chantrell, U. Atxitia, O. Chubykalo-Fesenko, S. El Moussaoui, L. Le Guyader, E. Mengotti, L. J. Heyderman, F. Nolting, A. Tsukamoto, A. Itoh, D. Afanasiev, B. A. Ivanov, A. M. Kalashnikova, K. Vahaplar, J. Mentink, A. Kirilyuk, T. Rasing, and A. V. Kimel, *Nat. Commun.* **3**, 666 (2012).
- ²⁰S. Mathias, C. La-O-Vorakiat, P. Grychtol, P. Granitzka, E. Turgut, J. M. Shaw, R. Adam, H. T. Nembach, M. E. Siemens, S. Eich, C. M. Schneider, T. J. Silva, M. Aeschlimann, M. M. Murnane, and H. C. Kapteyn, *Proc. Natl. Acad. Sci. USA* **109**, 4792 (2012).
- ²¹U. Atxitia, P. Nieves, and O. Chubykalo-Fesenko, *Phys. Rev. B* **86**, 104414 (2012).
- ²²J. H. Mentink, J. Hellsvik, D. V. Afanasiev, B. A. Ivanov, A. Kirilyuk, A. V. Kimel, O. Eriksson, M. I. Katsnelson, and Th. Rasing, *Phys. Rev. Lett.* **108**, 057202 (2012).
- ²³M. Plihal and D. L. Mills, *Phys. Rev. B* **58**, 14407 (1998).
- ²⁴M. S. S. Brooks, L. Nordstrom, and B. Johansson, *J. Phys.: Condens. Matter* **3**, 2357 (1991).